

The value of imaging techniques based on enhanced magnetic resonance imaging in the diagnosis and prediction response of radiotherapy for nasopharyngeal carcinoma

X. Liu¹, H. Pang¹, H. Zhou², J. Li³, X. Lu³, Y.R. Wang⁴, P. Zhou^{3*}, Y. Zhang^{1*}

¹Department of Oncology, The Affiliated Hospital of Southwest Medical University, Luzhou City, China

²Post-graduation Training Department, West China Hospital, Sichuan University, Luzhou City, China

³Department of Radiology, The Affiliated Hospital of Southwest Medical University, Luzhou City, China

⁴Nursing School Of Southwest Medical University, Luzhou City, China

ABSTRACT

► Original article

*Corresponding author:

Yan Zhang, M.D.,

Ping Zhou, M.D.,

E-mail:

zy258789@aliyun.com,

zhouping11@swmu.edu.cn

Received: April 2024

Final revised: July 2024

Accepted: August 2024

Int. J. Radiat. Res., April 2025;
23(2): 311-316

DOI: 10.61186/ijrr.23.2.8

Keywords: Magnetic resonance imaging; nasopharyngeal carcinoma; diagnosis; radiotherapy.

Background: To evaluate the value of imaging techniques based on enhanced magnetic resonance imaging (MRI) in diagnosing and predicting radiotherapy for nasopharyngeal carcinoma (NPC). **Materials and Methods:** This study analyzed 142 hospitalized patient's clinical data with nasopharyngeal carcinoma from March 2020 to December 2021. The patients were divided into valid and invalid groups. Preoperative T2 weighted image (T2WI) images were used for imaging analysis, feature texture parameters were screened based on R language, and a short-term efficacy prediction model for the training group and the validation group was constructed. **Results:** A total of 432 different texture parameters were obtained by T2WI image analysis of each patient and 5 characteristic texture parameters were obtained by Least Absolute Shrinkage and Selection Operator (LASSO) dimensionality reduction and 10-fold cross-validation screening. Specific examples were standard deviation, Cluster Prominence Angle 135 Offset 4, Correlation Angle 135 offset 4, Inertia Angle 135 Offset 4. The prediction models were constructed and the area under the receiver operating characteristic (ROC) curve of the training group model was 0.826 (95% Confidence intervals (CI): 0.708-0.944). The sensitivity and specificity were 83.67% and 69.14%, respectively. The area under the ROC curve of the validation group model was 0.810 (95% CI: 0.682-0.938) and the sensitivity and specificity were 89.46% and 63.29%, respectively. **Conclusion:** The prediction model constructed has high predictive accuracy, sensitivity and specificity for diagnosing nasopharyngeal carcinoma. The use of enhanced magnetic resonance imaging (MRI)-based imaging to predict the short-term outcome after radiotherapy for NPC was feasible and the prediction model was stable and reliable.

INTRODUCTION

Nasopharyngeal carcinoma (NPC) is a malignant tumor in the nasopharynx. Medical imaging technology is considered to be a non-invasive technology that generates images of internal tissues and organs of the human body, which can provide strong guidance for clinical analysis, diagnosis, and medical treatment. It aims to reveal the internal tissues and organs of the human body hidden under the skin and bones to help doctors diagnose diseases and develop therapeutic plans. About 85% of the world's nasopharyngeal cancer patients live in China, most of which are concentrated in Guangdong Province, so nasopharyngeal cancer is also known as "Canton Tumor" (1). Compared with other cancers of the head and neck, NPC is quite different in terms of symptoms, clinical manifestations, and treatment. The onset of nasopharyngeal cancer is insidious and

not easily detected, and early symptoms are not obvious. As a result, once diagnosed most patients (65-85%) have developed malignant nasopharyngeal carcinoma, which is not conducive for doctors to develop a treatment plan for their patients. According to relevant statistics, the distant metastasis rate of tumor cells in patients with NPC is as high as 25%-45% after radical radiotherapy (2-4). In the event of distant metastasis, the 5-year overall survival rate of patients will be significantly reduced to only 30%-40%. Therefore, distant metastasis is one of the main reasons for the failure of NPC treatment (5-7). For this reason, predicting the risk of distant metastases from nasopharyngeal cancer and developing timely, personalized and accurate treatment plans are essential for patient survival (8).

Due to the spatial and temporal heterogeneity of tumors, the application of genome or proteome detection techniques is limited (9). These techniques

require biopsy or invasive surgery to extract a small part of the tumor for analysis. The obtained features and indicators are not general and cannot be used for complete tumor feature analysis. Medical image is an important element to understanding medical science and disease diagnosis. Medical imaging is often adopted in clinical practice to diagnose tumors and guide the treatment of patients⁽¹⁰⁻¹¹⁾. Medical imaging technology can understand the internal situation of human tissues without damaging human tissues.

Magnetic resonance image (MRI) uses the proton content in human tissue to obtain the imaging information of the patient. Compared to X-ray and Computed Tomography (CT) images, MRI is multi-parameter imaging, which can provide more information for doctors to diagnose patients⁽¹²⁾. Both X-ray and CT images are tomographic images. The imaging principle of X-ray and CT image is through the different attenuation of X-ray passing through the object so as to obtain the imaging information of patients, which can clearly reflect the intensity of tissue, and the scanning speed is fast. More importantly, MRIs provide good resolution of human organs and tissues. However, doctors still have many deficiencies in their knowledge and analysis of medical images and rely too much on their own subjective experience. Therefore, how to use computer automation or semi-automation technology to diagnose medical images has become an important research topic. Imaging group (Radiomics) is a newly developed discipline in recent years and it has become a new development direction of medical imaging. Using many automated feature extraction algorithms, image data are transformed into a high-dimensional feature space that is easy to analyze and has been applied to diagnose, treat, and predict some tumours⁽¹³⁻¹⁵⁾. Among them, imaging has achieved good results in the application of lung cancer and breast cancer. In 2014, Aerts *et al.* adopted imaging features based on CT images of the lungs to analyze in depth the characteristics affecting the survival rate of patients with lung cancer⁽¹⁶⁾. Coroller *et al.* adopted imaging features to predict the risk of distant metastasis of lung cancer based on CT images of the lungs⁽¹⁷⁾. In 2016, Li *et al.* applied imaging features to analyze and predict the risk of breast cancer recurrence based on breast magnetic resonance images⁽¹⁸⁾. Although the research and application of imaging science have achieved some success in the diagnosis and treatment of some cancers, the research and application of imaging science in NPC is almost blank. In order to enhance the survival rate of patients with NPC, which has a high incidence of cancer in Guangdong, this paper discusses the value of imaging technology based on enhanced MRI in the diagnosis of NPC and the prediction of radiotherapy efficacy, which not only helps to fill the gaps in the research and application

of imaging in NPC, but also provides an effective diagnostic method in the clinic.

MATERIALS AND METHODS

General information

This study analyzed 142 hospitalized patients with nasopharyngeal carcinoma clinical data from March 2020 to December 2021. The patients were divided into a training group and validation group, and preoperative T2 weighted image (T2WI) images were used for imaging analysis, and feature texture parameters were screened based on R language (New Zealand), and a short-term efficacy prediction model for the training group and the validation group was constructed. There were 81 males and 61 females (24 to 83 years old, 58.78 ± 10.06 years). All patients were confirmed by pathology and underwent MRI scanning before the operation. This study was permitted by the Medical Ethics Association of our hospital, and all patients were given informed consent (Approve number: KY2023041).

Selection criteria: (1) regardless of sex, age from 20 to 85 years old; (2) NPC was diagnosed clinically and confirmed by pathology; (3) MRI scan was performed within 1 month before radiotherapy and imaging follow-up was performed within 3 to 4 months after treatment; (4) single focus (maximum diameter 3~7cm), multiple lesions (≤ 3 , maximum diameter ≤ 7 cm); (5) there was no tumor thrombus in the portal vein and hepatic vein; (6) physical condition was good, Karnofsky score ≥ 70 points.

Exclusion criteria: (1) the patients were not followed up regularly; (2) the clinical data were incomplete; (3) there were artefacts in the images, which affected the observation of the lesions.

Treatment methods

Evaluation of curative effect

The short-term efficacy of transcatheter arterial chemoembolization (TACE) was evaluated according to the modified response evaluation criteria in solid tumors (MRECIST)⁽¹⁹⁾, as follows: (1) complete remission (CR): enhancement of intratumoral arteries disappeared in all target lesions; (2) partial remission (PR): the size of the target lesion or the sum of all diameters of the enhanced lesion is reduced by at least 30%; (3) Disease stability (SD): the minimum diameter of the target lesion does not reach the PR, and the degree of enlargement does not meet the diameter requirements of disease progression; (4) Disease progression (PD): the size of the tumor (the sum of the diameters of all the enhanced lesions of the target focus and the maximum diameter of the focus) increases by at least 20%, or new lesions appear. In this study, patients with CR and PR were considered to be effective in the short term, while patients with SD and PD were

considered ineffective. 61 patients were found to be effective and 62 patients were ineffective.

Grouping

The patients were arbitrarily assigned to the training group (n=96) and verification group (n=46). There were 32 effective and 64 ineffective patients in the training group, 23 effective and 23 ineffective patients in the verification group. There exhibited no significant difference.

Preoperative MRI scanning method

MRI examined all patients before the operation. The instrument was a Philips INGENIA 3.0 T MR scanner, which contained T2WI sequence. The patients underwent no contrast-enhanced image examination within 48 hours and fasted within 4 hours before the examination. Before scanning, the patients were instructed to carry out breathing training, hold their breath at the end of the breath and check in the supine position. The specific scanning parameters were as follows: TR1086ms, TE80ms, flip angle 90°, layer thickness 5mm, layer spacing 1mm, matrix 408×408, visual field 400mm×400mm, voxel size 1.1mm×1.1mm×5.0mm. The segmented collection: collection times or average times 1, parallel acquisition factor 2.

1.2.4 Image texture feature extraction and dimensionality reduction. The T2WI images of all patients in the training and verification group were analyzed using imageology, and 432 different texture parameters were obtained. The above 396 texture feature parameters were preprocessed, and all outliers in the parameters were replaced by the median, which carried on the standardization processing of Z-score. R language was adopted to reduce the dimension of LASSO, and 10-fold cross-validation and texture parameters were modeled using a multiple logistic regression analysis.

Modeling and statistical analysis

All statistical data were analyzed with R language (Version:3.4.4, <https://www.r-project.org/>). Based on the radiation value of each patient, the prediction models of training group and verification group were constructed by multiple Logistic regression and the stability and accuracy of the two models were evaluated.

RESULTS

The general data between the operation and verification group

There were no differences in age, sex, history of hepatitis B, alanine aminotransferase, aspartate transaminase, glutamyl transpeptidase, alkaline phosphatase, total bilirubin, albumin, plasma prothrombin time and alpha-fetoprotein ($P>0.05$), (tables 1 and 2). The typical imaging images of

patients before and after treatment are indicated in figure 1. 2 weeks before treatment, the length of the focus was 26.35mm. Three months after treatment, the long diameter of the focus was 28.94mm. One week before treatment, the long diameter of the focus was 52.70mm, which was basically inactivated 3.5 months after the operation.

Table 1. The general data of patients in operation group was normal.

| Group | Valid group (n=32) | Invalid group (n=64) | t/ χ^2 | P |
|----------------------------------|--------------------|----------------------|-------------|-------|
| Age (years) | 58.29±17.76 | 59.48±17.33 | 0.315 | >0.05 |
| Gender (male / female) | 18/14 | 35/29 | 0.021 | >0.05 |
| Alanine Transaminase (U/L) | 45.26±14.17 | 45.03±43.51 | 0.029 | >0.05 |
| Aspartate aminotransferase (U/L) | 57.36±18.07 | 57.63±17.98 | 0.069 | >0.05 |
| Glutamyl transpeptidase (U/L) | 119.54±115.03 | 119.61±113.56 | 0.003 | >0.05 |
| Alkaline phosphatase (U/L) | 147.65±82.41 | 148.97±81.03 | 0.075 | >0.05 |
| Total bilirubin(μ mol/L) | 25.43±66.17 | 25.51±64.82 | 0.006 | >0.05 |
| Albumen (g/L) | 35.06±4.17 | 35.81±4.08 | 0.843 | >0.05 |
| Plasma prothrombin time (s) | 13.17±1.56 | 13.28±1.34 | 0.359 | >0.05 |
| Alpha fetoprotein (μ g/L) | 432.84±108.56 | 397.21±87.51 | 1.733 | >0.05 |

Table 2. The general data of patients in verification group was normal.

| Group | Valid group (n=23) | Invalid group (n=23) | t/ χ^2 | P |
|----------------------------------|--------------------|----------------------|-------------|-------|
| Age (years) | 55.63±13.45 | 56.27±13.08 | 0.164 | >0.05 |
| Gender (male / female) | 15/8 | 13/10 | 0.365 | >0.05 |
| Alanine transaminase (U/L) | 58.12±6.12 | 58.83±7.01 | 0.366 | >0.05 |
| Aspartate aminotransferase (U/L) | 63.54±50.02 | 63.41±51.32 | 0.009 | >0.05 |
| Glutamyl Transpeptidase (U/L) | 196.87±154.21 | 197.69±155.06 | 0.018 | >0.05 |
| alkaline phosphatase (U/L) | 152.54±53.06 | 155.61±54.73 | 0.193 | >0.05 |
| Total bilirubin (μ mol/L) | 25.38±66.17 | 25.61±64.08 | 0.012 | >0.05 |
| Albumen (g/L) | 35.19±4.51 | 35.44±4.03 | 0.198 | >0.05 |
| Plasma prothrombin time (s) | 13.06±1.51 | 13.25±1.28 | 0.460 | >0.05 |
| Alpha fetoprotein(μ g/L) | 432.19±243.03 | 428.48±235.61 | 0.053 | >0.05 |

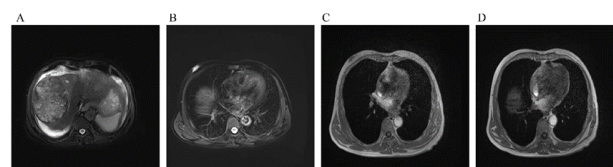


Figure 1. Typical cross-sectional T2WI of NPC patients with different prognosis after radiotherapy and chemotherapy. **A:** The male was 68 years old, 2 weeks before treatment, the length of the focus was 26.35mm. **B:** three months after treatment, the long diameter of the focus was 28.94mm. **C:** The male was 42 years old, one week before treatment. The long diameter of the focus was 52.70mm, **D:** the focus was basically inactivated 3.5 months after operation. Note: T2WI: T2 weighted image; NPC: nasopharyngeal carcinoma.

Texture feature screening

After dimensionality reduction analysis, five texture parameters with the strongest significance were obtained (std Deviation, Cluster Prominence

Angle 135 Offset 4, Correlation Angle 135 offset 4, Inertia Angle 135 Offset 4, Inverse Difference Moment Angle 45 Offset 4). The results of dimensionality reduction were indicated in figures 2A and 2B. Based on the above five texture features, each patient's corresponding radiation value (Rad scores) was calculated and the bar chart showed that the patients with different prognoses in the training group and the verification group could be clearly distinguished (figure 2C ~ 2D).

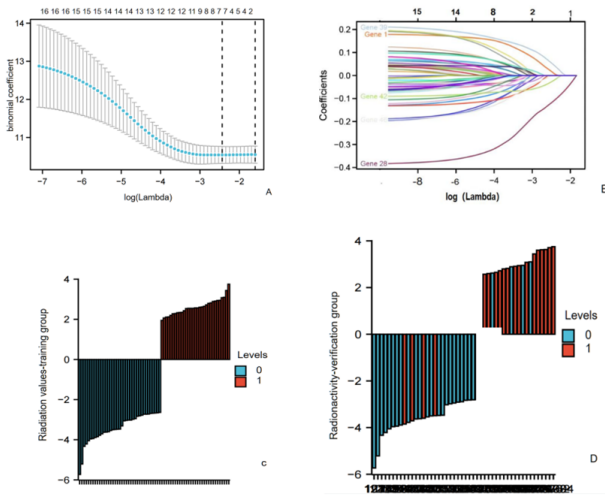


Figure 2. Dimensionality reduction process of texture parameters and corresponding bar graph. **A:** Using LASSO regression and cross validation to reduce the dimension, there were 5 features corresponding to the minimum error; **B:** the number of corresponding parameters and the change of coefficient value in the case of different λ values; **C:** the bar chart of the training group; **D:** the bar chart of the verification group Note: LASSO: Least Absolute Shrinkage and Selection Operator.

Model prediction efficiency:

The area under the subject working characteristic (ROC) curve of the training group model was 0.826 (95% CI: 0.708-0.944). The sensitivity and specificity were 83.67% and 69.14%, respectively. The area under the ROC curve of the verification group model was 0.810 (95% CI: 0.682~0.938). The sensitivity was 89.46% and the specificity was 63.29%. The model's ROC curve in the training and verification groups was indicated in figures 3 and 4. The calibration curve of the model was indicated in figures 5A and 5B. The calibration curve showed that the prediction probability of the model in the training group and verification group was close to the actual probability.

Figure 3. Working characteristic (ROC) curve of subjects in training group. Note: ROC: receiver operating characteristic.

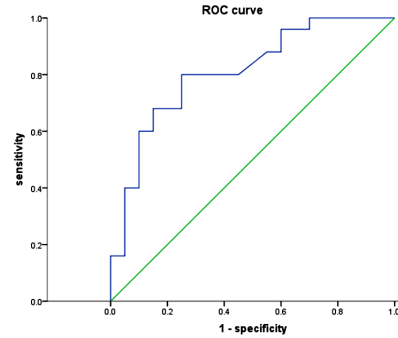
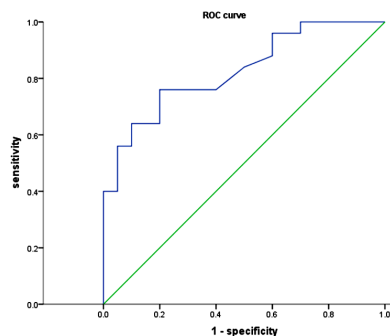


Figure 4. ROC curve of verifying group subjects.

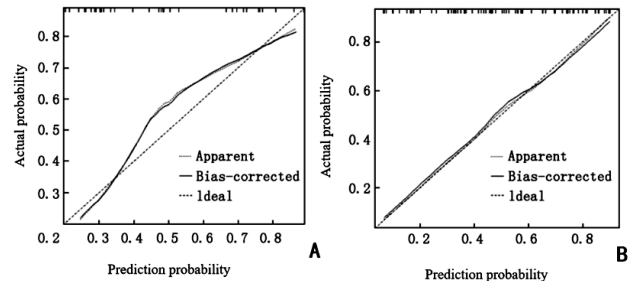


Figure 5. Calibration curve of NPC patients in training group and verification group. **A:** the corresponding correction curve of the training group; **B:** the corresponding correction curve of the verification group. Note: NPC: nasopharyngeal carcinoma.

DISCUSSION

In order to enhance the survival rate of patients with NPC, which has a high incidence of cancer in Guangdong, this paper discusses the value of imaging technology based on enhanced MRI in diagnosing NPC and predicting radiotherapy efficacy. Medical imaging is a subject of visual expression technology that can present the internal tissues and organs of the human body (19). According to the World Health Organization, NPC incidence in South China, with Guangzhou as the centre, is much higher than in other regions (40-100 times higher than in Europe and North America). As a scientific research field, medical imaging, including X-ray imaging, MRI, ultrasonic imaging, tactile imaging, thermal spectrum imaging and nuclear medicine functional imaging, is widely adopted in medical diagnosis and clinical treatment. Until 2010, there have been more than 500 million medical images in the world (20).

MRI is another major progress and breakthrough in medical imaging after CT. Since physicists Peter Mansfield and Paul Lauterbur invented magnetic resonance technology in the late 1970s, it is estimated that more than 25,000 nuclear magnetic resonance scanners are in use worldwide (21). Although the harm of X-rays can be well controlled in most medical environments, MRI is still considered to be a better choice than CT and has been widely adopted in hospitals and clinics for medical diagnosis, disease staging, and follow-up examination.

In recent years, radiology has become a new development in medical imaging (22,23). It transforms medical image data into a high-dimensional feature space that is easy to analyze through many automatic

feature extraction algorithms. These extracted features are called imaging features, which can discover and reveal disease features that cannot be observed with the naked eye⁽²⁴⁾. Imaging science is expected to find distinct medical image features of different disease types to predict diagnosis and observe the clinical response after treatment so as to provide valuable information for accurate individualized treatment^(25,26). Imaging science first appeared in the field of tumor treatment, and it has also achieved great success in the field of tumor treatment. For example, Wang *et al.* based on breast magnetic resonance images applied imaging features to analyze and predict the risk of breast cancer recurrence⁽²⁷⁾. Wu *et al.* Lung-based CT images used imaging features to deeply analyzed the characteristics affecting lung cancer patients' survival rate⁽²⁸⁾. Xu *et al.*, based on the CT images of the lungs, used imaging features to predict the risk of distant metastasis of lung cancer⁽²⁹⁾.

In this study, five texture parameters that were highly related to the prognosis of the disease were screened using an imaging method, and a radiotherapy prognosis prediction model of NPC was constructed. The above five texture parameters also have some clinical significance, among which is std Deviation, which is a measure adopted to quantify the change or dispersion of a group of data values. The process of using images is assigned into several processes, including: 1) image acquisition. The underlying medical images adopted to describe tumors are obtained using medical scanning techniques, including CT and MRI mentioned above. The raw data obtained by medical scanning must be further processed before it can be used for medical research and clinical diagnosis. Various effective imaging methods should be chosen for different diseases and research situations. Even if it is the same imaging method, we should try different parameters to obtain the best medical image effect. For example, the medical image data is the magnetic resonance image data of NPC in this study and the images of each patient with NPC are classified into three groups: spin echo (Spin Echo) images captured by T1, T1C and T2 weighted images. Medical image data is precious and it is difficult to collect images of many diseases. Therefore, the collected medical images (desensitized) should be saved in a large database and accessible to all hospitals. Extensive cooperation and accumulation of work are the basis of the research of big data in medical images; 2) image segmentation. After the image is collected, the image should be further processed to obtain the part that is meaningful for theoretical research and clinical diagnosis (usually the focus area, in this study is the NPC tumor area), this part is called the "region of interest" (ROI). In order to obtain the region of interest, it is necessary to segment the image. Nowadays, there are a large number of algorithms for

automatic detection and segmentation of focus areas. However, these algorithms often have limitations and can only be used in specific diseases or cases with clear edges of lesions. With the development of deep learning, the algorithm of automatic segmentation of focus regions by deep learning is being improved. The research in this area still has a long way to go. To improve the reliability and accuracy of the results of this study, the tumor area of nasopharyngeal carcinoma used in this study was outlined manually by the oncologist. On this basis, we segment the tumor region; 3) feature extraction and screening. After the segmentation of the focus region is completed, the 3D matrix and 3D model of the focus region can be constructed. According to the 3D matrix and 3D model, many features of the tumor can be calculated. These features include volume, surface area, shape, density, grayscale intensity, texture, tumor location and relationship with surrounding tissues. Due to the wide variety of data features, it is necessary to limit the data to eliminate redundant information. Therefore, it is also very necessary to screen or reduce the dimension of features; 4) analysis. After the data features are screened, it is necessary to analyze the data effectively. Prior to the actual analysis, the corresponding clinical and molecular data needs to be integrated, sometimes even using genetic data. In addition to the imaging data of patients with NPC, this study also provided the corresponding clinical diagnostic data and molecular and cellular level examination data. These data can provide great help and guidance for practical research and analysis. There are many ways to analyze data, and for example, you can compare whether different features contain the same information and then reveal what they mean when they appear. In addition, supervised analysis or unsupervised analysis can be adopted⁽³⁰⁾. Supervised analysis uses clinical diagnostic data or molecular data as outcome variables to create a predictive model. The unsupervised analysis does not rely on additional data; it directly analyzes and summarizes the characteristic information of imaging science in a visualized form. In this way, the results of the analysis can be clearly observed.

Cluster Prominence is a measure of distributed asymmetric data and the high value of this feature indicates that the image has low symmetry, correlation measures the similarity of gray levels in adjacent pixels to express the correlation between pixels and their adjacent pixels in the whole image. Inertia reflects the clarity of the image and the depth of the texture groove. Inverse Difference Moment is a gray co-occurrence matrix (GLCM) texture parameter, representing the joint probability of some groups of pixels with certain gray values. They reflect the image heterogeneity in different aspects and imply the relevant information about the development of tumor lesions after radiotherapy for

NPC. In this study, the area under ROC curve of training and verification group was as high as 0.826 and 0.810 respectively. In addition, the sensitivity and specificity were high, which showed that the model had higher prediction ability. Compared with other prognostic methods, the method of texture analysis is more convenient and can achieve non-invasive prediction before operation. For the patients with poor radiotherapy effect of NPC, we can avoid more harm caused by clinical wrong decision and make a more reasonable treatment plan for patients. This study also has some shortcomings. The quality of the study is limited due to the small sample size of this study. In addition, this study is a single-center study, and the results may be biased. Therefore, the results of this study may differ from the results of other large-scale multicenter studies. However, this study still has important clinical significance, and further in-depth studies will be conducted in the future.

CONCLUSION

The prediction model constructed in this study is reliable, indicating that using MRI texture analysis technology to construct the short-term curative effect prediction model of NPC after radiotherapy is feasible.

Funding: No funding.

Conflicts of interests: There were no conflicts of interests of all authors.

Ethical consideration: The study was approved by the hospital's ethics committee.

Author contribution: X.L., H.P., P.Z. and Y.Z. co-designed the study. X.L. and H.P. conducted the study. H.Z., J.L., X.L. and Y.R.W. helped and advised on this study. X.L. and H.P. analyzed the data. All authors contributed to the editorial revision of the manuscript. All authors read and approved the final manuscript. All authors participated fully in the work and agreed to take responsibility for all aspects of the work.

REFERENCES

1. Tsang CM, Lui VW, Bruce JP, et al. (2020) Translational genomics of nasopharyngeal cancer. *Semin Cancer Biol*, **61**: 84-100.
2. Lee A, Chow JC, Lee NY (2021) Treatment deescalation strategies for nasopharyngeal cancer: a review. *JAMA Oncol*, **7**: 445-53.
3. Salehiniya H, Mohammadian M, Mohammadian-Hafshejani A, et al. (2018) Nasopharyngeal cancer in the world: epidemiology, incidence, mortality and risk factors. *WCRJ*, **5**: e1046.
4. Chan AT, Hui EP, Ngan RK, et al. (2018) Analysis of plasma Epstein-Barr virus DNA in nasopharyngeal cancer after chemoradiation to identify high-risk patients for adjuvant chemotherapy: a randomized controlled trial. *J Clin Oncol*, **36**: 3091-100.
5. Dong D, Zhang F, Zhong LZ, et al. (2019) Development and validation of a novel MR imaging predictor of response to induction chemotherapy in locoregionally advanced nasopharyngeal cancer: a randomized controlled trial substudy (NCT01245959). *BMC Med*, **17**(1): 190.
6. Li S, Xiao J, He L, et al. (2019) The tumor target segmentation of nasopharyngeal cancer in CT images based on deep learning methods. *Technol Cancer Res Treat*, **18**: 1533033819884561.
7. Lin D, Wu Q, Qiu S, et al. (2019) Label-free liquid biopsy based on blood circulating DNA detection using SERS-based nanotechnology for nasopharyngeal cancer screening. *Nanomedicine*, **22**: 102100.
8. Spadarella G, Calareso G, Garanzini E, et al. (2021) MRI based radiomics in nasopharyngeal cancer: Systematic review and perspectives using radiomic quality score (RQS) assessment. *Eur J Radiol*, **140**: 109744.
9. Yarza R, Bover M, Agulló-Ortuño MT, et al. (2021) Current approach and novel perspectives in nasopharyngeal carcinoma: The role of targeting proteasome dysregulation as a molecular landmark in nasopharyngeal cancer. *J Exp Clin Cancer Res*, **40**(1): 1-8.
10. Huang S, Cao B, Zhang J, et al. (2021) Induction of ferroptosis in human nasopharyngeal cancer cells by cucurbitacin B: molecular mechanism and therapeutic potential. *Cell Death Dis*, **12**(3): 237.
11. Hui EP, Ma BB, Lam WJ, et al. (2021) Dynamic Changes of Post-Radiotherapy Plasma Epstein-Barr virus DNA in a randomized trial of adjuvant chemotherapy versus observation in nasopharyngeal cancer. *Clin Cancer Res*, **27**(10): 2827-2836.
12. Jiří K, Vladimír V, Michal A, et al. (2021) Proton pencil-beam scanning radiotherapy in the treatment of nasopharyngeal cancer: dosimetric parameters and 2-year results. *Eur Arch Otorhinolaryngol*, **278**(3): 763-769.
13. Blanchard P, Biau J, Huguet F, et al. (2022) Radiotherapy for nasopharyngeal cancer. *Cancer Radiother*, **26**(1-2): 168-173.
14. Liao KC, Chuang HC, Chien CY, et al. (2021) Quality of life as a mediator between cancer stage and long-term mortality in nasopharyngeal cancer patients treated with intensity-modulated radiotherapy. *Cancers*, **13**(20): 5063.
15. Spadarella G, Calareso G, Garanzini E, et al. (2021) MRI based radiomics in nasopharyngeal cancer: Systematic review and perspectives using radiomic quality score (RQS) assessment. *Eur J Radiol*, **140**: 109744.
16. Aerts HJ, Velazquez ER, Leijenaar RT, et al. (2014) Decoding tumour phenotype by noninvasive imaging using a quantitative radiomics approach. *Nat Commun*, **5**: 4006.
17. Coroller TP, Grossmann P, Hou Y, et al. (2015) CT-based radiomic signature predicts distant metastasis in lung adenocarcinoma. *Radiother Oncol*, **114**(3): 345-350.
18. Li H, Zhu Y, Burnside ES, et al. (2016) MR imaging radiomics signatures for predicting the risk of breast cancer recurrence as given by research versions of MammaPrint, Oncotype DX, and PAM50 gene assays. *Radiology*, **281**(2): 382-391.
19. Allam AP, Ali Hassan HG, Mohamed BA. (2021) Role of CT and modified response evaluation criteria in solid tumors (RECIST criteria) in response evaluation of malignant pleural mesothelioma. *QJM*, **114**(Supplement-1): hcab106-018.
20. Lee S, Choi Y, Seo MK, et al. (2022) Magnetic resonance imaging-based radiomics for the prediction of progression-free survival in patients with nasopharyngeal carcinoma: A systematic review and meta-analysis. *Cancers*, **14**: 653.
21. Hou J, Li H, Zeng B, et al. (2022) MRI-based radiomics nomogram for predicting temporal lobe injury after radiotherapy in nasopharyngeal carcinoma. *Eur Radiol*, **32**(2): 1106-1114.
22. Wu X, Dong D, Zhang L, et al. (2021) Exploring the predictive value of additional peritumoral regions based on deep learning and radiomics: a multicenter study. *Med Phys*, **48**(5): 2374-2385.
23. Bao D, Zhao Y, Liu Z, et al. (2021) Prognostic and predictive value of radiomics features at MRI in nasopharyngeal carcinoma. *Discov Oncol*, **12**(1): 63.
24. Duan W, Xiong B, Tian T, et al. (2022) Radiomics in nasopharyngeal carcinoma. *Clin Med Insights Oncol*, **16**: 11795549221079186.
25. Yan C, Shen DS, Chen XB, et al. (2021) CT-based radiomics nomogram for prediction of progression-free survival in locoregionally advanced nasopharyngeal carcinoma. *Cancer Manag Res*, **2021**: 6911-23.
26. Lam SK, Zhang J, Zhang YP, et al. (2022) A multi-center study of CT-based neck nodal radiomics for predicting an adaptive radiotherapy trigger of ill-fitted thermoplastic masks in patients with nasopharyngeal carcinoma. *Life*, **12**: 241.
27. Wang Y, Li C, Yin G, et al. (2022) Extraction parameter optimized radiomics for neoadjuvant chemotherapy response prognosis in advanced nasopharyngeal carcinoma. *Clin Transl Radiat Oncol*, **33**: 37-44.
28. Wu S, Li H, Dong A, et al. (2021) Differences in radiomics signatures between patients with early and advanced T-stage nasopharyngeal carcinoma facilitate prognostication. *J Magn Reson Imaging*, **56**(1): 221-222.
29. Wu S, Li H, Dong A, et al. (2021) Differences in radiomics signatures between patients with early and advanced T-stage nasopharyngeal carcinoma facilitate prognostication. *Magn Reson Imaging*, **56**(1): 221-222.
30. Bao D, Liu Z, Geng Y, et al. (2022) Baseline MRI-based radiomics model assisted predicting disease progression in nasopharyngeal carcinoma patients with complete response after treatment. *Cancer Imaging*, **22**(1): 10.